Available online at www.sciencedirect.com
SCIENCE DIRECT®
International Journal of Heat and Fluid Flow 25 (2004) 945–960
International Journal of HEAT AND FLUID FLOW
www.elsevier.com/locate/ijhff

An investigation of the heat transfer and static pressure on the over-tip casing wall of an axial turbine operating at engine representative flow conditions. (II). Time-resolved results

S.J. Thorpe [a,*], S. Yoshino [b,1], R.W. Ainsworth [a], N.W. Harvey [c]

[a] Department of Engineering Science, University of Oxford, Parks Road, Oxford OX1 3PJ, UK
[b] Tokyo Electric Power Company, Thermal Power Technology Group, 4-1 Egasaki-cho, Tsurumi-ku, Yokohama, 230-8510, Japan
[c] Rolls-Royce plc, Turbine Systems (PCF-2), PO Box 31, Derby, DE23 6AY, UK

Received 17 November 2003; accepted 20 February 2004
Available online 20 May 2004

Abstract

This article reports the measurements of time-resolved heat transfer rate and time-resolved static pressure that have been made on the over-tip casing of a transonic axial-flow turbine operating at flow conditions that are representative of those found in modern gas turbine engines. This data is discussed and analysed in the context of explaining the physical mechanisms that influence the casing heat flux. The physical size of the measurement domain was one nozzle guide vane-pitch and from −20% to +80% rotor axial chord. Additionally, measurements of the time-resolved adiabatic wall temperature are presented. The time-mean data from the same set of experiments is presented and discussed in Part I of this article. The nozzle guide vane exit flow conditions in these experiments were a Mach number of 0.93 and a Reynolds number of 2.7×10^6 based on nozzle guide vane mid-height axial chord. The data reveal large temporal variations in heat transfer characteristics to the casing wall that are associated with blade-tip passing events and in particular the blade over-tip leakage flow. The highest instantaneous heat flux to the casing wall occurs within the blade-tip gap, and this has been found to be caused by a combination of increasing flow temperature and heat transfer coefficient. The time-resolved static pressure measurements have enabled a detailed understanding of the tip-leakage aerodynamics to be established, and the physical mechanisms influencing the casing heat load have been determined. In particular, this has focused on the role of the unsteady blade lift distribution that is produced by upstream vane effects. This has been seen to modulate the tip-leakage flow and cause subsequent variations in casing heat flux. The novel experimental techniques employed in these experiments have allowed the measurement of the time-resolved adiabatic wall temperature on the casing wall. These data clearly show the falling flow temperatures as work is extracted from the gas by the turbine. Additionally, these temperature measurements have revealed that the absolute stagnation temperature within the tip-gap flow can be above the turbine inlet total temperature, and indicates the presence of a work process that leads to high adiabatic wall temperatures as a blade-tip passes a point on the casing wall. It is shown that this phenomena can be explained by consideration of the flow vectors within the tip-gap, and that these in turn are related to the local blade loading distribution. The paper also assesses the relative importance of different time-varying phenomena to the casing heat load distribution. This analysis has indicated that up to half of the casing heat load is associated with the over-tip leakage flow. Finally, the implications of the experimental findings are discussed in relation to future shroudless turbine design, and in particular the importance of accounting for the high heat fluxes found within the tip-gap.

Keywords: Heat transfer; Turbine; Tip leakage; Aerothermodynamics; Transonic; Thin-film gauge

1. Introduction

Part I of this work (Thorpe et al., 2004) reports the time-mean heat transfer and static pressure distributions that have been measured on the over-tip casing of a transonic axial-flow turbine rotor operating at flow conditions that are representative of those found in

* Corresponding author. Tel.: +44-1865-288735; fax: +44-1865-288756.
E-mail address: steve.thorpe@eng.ox.ac.uk (S.J. Thorpe).
[1] Currently at Tokyo Electric Power Company, Tokyo, Japan.

0142-727X/$ - see front matter © 2004 Elsevier Inc. All rights reserved.
doi:10.1016/j.ijheatfluidflow.2004.02.028

Nomenclature

c	specific heat capacity
C_{ax}	axial chord length
v	flow velocity in blade relative frame
H	enthalpy
U	blade tip velocity
V	flow velocity in absolute frame
Greeks	
α	flow angle in absolute frame
δ	flow angle in blade relative frame
Subscripts	
aw	adiabatic wall
o	total conditions
pass	relating to the blade passage flow
tip	relating to the blade tip gap flow
w	wall
2	nozzle guide vane exit conditions
θ	circumferential direction

modern gas turbine engines. A brief overview of the major findings will be given here in order to aid overall understanding. The time-mean data show that the heat flux to the casing wall falls with increasing axial position through the rotor due to a reduction in both the flow recovery temperature and the local Nusselt number. The time-mean Nusselt number falls by 36% between the rotor inlet plane and 80% axial-chord. In contrast to the large axial variations in heat transfer, only small circumferential variations have been observed in the time-mean data, indicating the relatively small influence of the upstream nozzle guide vanes on the time-mean flow conditions adjacent to the over-tip casing wall. However, enhanced levels of heat transfer and static pressure have been seen in the vicinity of the nozzle guide vane trailing edge and rear part of the suction surface. The current article (Part II) presents the time-resolved data that was acquired during the same set of experiments as the time-mean data. These data provide considerable insight into the physical mechanisms that influence the casing heat load and have allowed a more fundamental understanding of the fluid dynamics to be established.

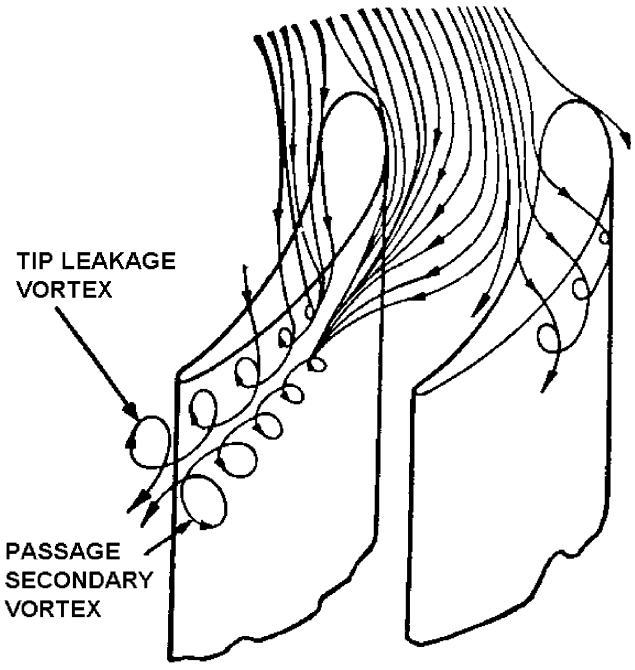

Fig. 1. A schematic diagram that illustrates the basic over-tip leakage flow phenomena.

1.1. The basic over-tip leakage flow physics

The flow-field adjacent to the over-tip casing of an axial-flow turbine presents a most complicated fluid dynamic problem that involves high-speed unsteady aerodynamics, large work processes and attendant total temperature changes (the absolute total temperature drops by approximately 90 K in the Oxford turbine). A schematic diagram of the over-tip leakage flow is presented in Fig. 1. As the transonic flow adjacent to the casing wall exits the nozzle guide vanes, it traverses the vane–blade axial gap and comes increasingly under the influence of the moving blade potential field; here, it experiences blade periodic pressure fluctuations that inevitably cause modification to the casing boundary layer. The frequency of these blade passing events is typically in the range 5–20 kHz, depending upon the shaft speed and the number of blades (8.9 kHz in the case of the Oxford turbine). As the flow adjacent to the casing wall advances toward the blade passage inlet plane, the picture is further complicated by the direct blade passing events that periodically disturb the casing boundary layer. These disturbances are due to the high fluid velocities found in the tip leakage flow and lead to higher convective heat transfer coefficients as the blade-tip passes. The tip leakage flow is produced by the pressure difference across the blade-tip, and changes as a function of axial distance through the turbine. Consequently, the tip leakage flow itself varies along the length of the blade-tip, and may be supersonic in both the absolute and relative frames of reference, depending upon the local pressure ratio across the tip. The direction of the tip-leakage flow is also a function of position

on the blade-tip, as dictated by the pressure distribution around the blade. At a given point on the stationary casing wall, the boundary layer is never truly steady, but instead is modulated at the blade passing frequency by the imposed fluctuations of the effective free-stream velocity, density and (as will be shown in Section 2) recovery temperature. As can be appreciated, the flow physics and heat transfer present in this experimental study are particularly complicated, involving unsteady transonic phenomena; however, it is through the interpretation of the time-resolved measurements that a significant improvement in both the qualitative and quantitative understanding of the blade/casing interaction has been achieved, and is reported here.

1.2. Experimental approach

The experiments reported in this article were performed in the transonic axial-flow turbine test facility located at the Department of Engineering Science in the University of Oxford. This short duration facility has been employed in the investigation of various aspects of the aero-thermodynamics of axial flow turbines for more than 15 years (Ainsworth et al., 1988; Garside et al., 1994; Miller et al., 2003). In the current investigation the facility was fitted with extensive over-tip casing wall instrumentation for the measurement of heat transfer rate and static pressure. For full details of the experimental techniques and background to this work, the reader is directed to Part I (Thorpe et al., 2004): only a brief description of the test facility and instrumentation will be provided here.

1.2.1. The measurement of time-resolved heat transfer rate and adiabatic wall temperature

The heat transfer rate distribution to the over-tip casing wall has been measured using thin-film platinum resistance gauges mounted on a semi-infinite ceramic substrate. The size of the gauges is 1×0.08 mm. A total of 56 measurement locations have been employed that cover one vane-pitch and from −20% to +80% rotor axial chord, and are arranged on a regular 7×8 array. Fig. 2 shows a schematic diagram of the measurement locations relative to the upstream vane and blade-tips.

The unsteady nature of the heat flux to the over-tip casing wall is caused by the blade periodic modulation of the flow conditions immediately adjacent to it. The impact of this can be summarised as causing the following physical effects:

- A temporal variation in Nusselt number that is produced by the time-varying velocity and pressure fields immediately above the casing wall.
- A temporal variation in flow total temperature that is related to the distribution of work production (energy extraction) through the blade row.

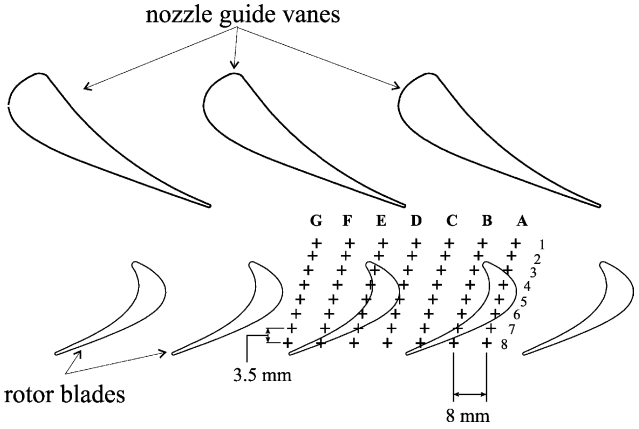

Fig. 2. A schematic diagram that illustrates the position of the casing wall instrumentation relative to the upstream guide vanes and rotor blade row.

The measurement of heat flux alone is not sufficient to define the relative importance of these two effects: it is of paramount importance to measure time-resolved adiabatic wall temperature as well as time-resolved heat flux. To this end, a heat transfer measurement scheme was devised that enables the variation of heat flux to be determined as a function of the local wall temperature (see Thorpe et al., 2004). This information enables the blade-periodic (deterministic) variation in the adiabatic wall temperature to be established for each measurement location.

Some clarification of the meaning of this measurement parameter is required. As has already been acknowledged, the over-tip casing boundary layer is not steady. It is greatly influenced by the moving pressure field produced by the blades, and is subjected to fierce disturbance from the over-tip leakage flow which causes variations in both flow speed and direction immediately adjacent to the casing wall. Consequently, the boundary layer state is continuously changing in response to these changes in the flow conditions at the blade passing frequency. Potentially, this implies that non-equilibrium conditions may exist within the boundary layer (actually, in both the momentum and thermal boundary layers). However, if the response time of the boundary layer is sufficiently fast, the assumption of a quasi-steady boundary layer is valid. In this case, the boundary layer can be considered to pass through a succession of equilibrium states, and the boundary layer responds more rapidly than the time-scale of the imposed fluctuations. Schlichting and Gersten (2000) have considered the response time of the a flat-plate boundary layer that is exposed to fluctuations in free-stream conditions, and determined the conditions under which the quasi-steady assumption is valid. For the thin, high-speed boundary layers found in high-speed turbines the response time is very short (a few microseconds) and relatively large

amplitude fluctuations can be tolerated. The flat-plate case considered by Schlichting and Gersten (2000) indicates that for frequencies of at least 100 kHz, the casing boundary layer can be considered quasi-steady.

1.2.2. The measurement of time-resolved static pressure

The unsteady static pressure distribution on the casing wall has been measured using fast-response semiconductor pressure sensors (manufactured by Kulite Semiconductor Inc.). These pressure measurements were made at precisely the same locations on the casing wall as the heat transfer measurements, and are defined in Fig. 2. The effective bandwidth of the pressure measurements was 100 kHz.

2. Experimental results

2.1. Data processing and presentation

The flow conditions near the casing wall are modulated at the blade-passing frequency (8.9 kHz), and consequently the heat transfer and static pressure measurements contain frequency components that correspond to this disturbance. The measurements of unsteady heat transfer and static pressure can be considered to consist of three fundamental components:

- *Time-mean*. This data is presented in Part I of this work.
- *Deterministic unsteady*. This is the time-resolved fluctuation that is related to the blade-passing period, and is exactly repeated for each blade-passing cycle.
- *Random unsteady*. This is the time-unresolved fluctuation and is caused by random features in the flow, such as turbulence.

The current work concerns the deterministic unsteady component of the time-resolved measurements. To this end, the measurements of unsteady heat transfer rate and static pressure have been analysed by employing a phase-locked averaging technique. This approach reduces the time-resolved data into a sequence of individual blade-passing events which are averaged to produce a characteristic unsteady measurement that covers one blade-passing cycle. The data reduction algorithm has utilised the data from two complete revolutions of the rotor disk and therefore uses 120 blade-passing events to form the phase-locked average signal.

The series of experiments has generated a large database of casing wall measurements that reveal the temporal and spatial variations in static pressure and heat flux. The data presented below is by necessity a small subset of the total measurements obtained. However, this data captures the important features of the over-tip casing aerodynamics, and amply illustrates the unsteady nature of the flow regime and how this influences the heat transfer. The data is presented as a sequence of contour plots at increments of the blade passing cycle. One such cycle is defined as the time taken for adjacent blades to pass the trailing edge of a vane, and is referred to in units of blade-phase which ranges between 0% and 100%. Note that 0% blade-phase is defined as the position when a blade leading edge is axially aligned with a vane trailing edge. Positions relative to the vanes are defined in terms of vane-pitch, which ranges between 0% and 100%, with the 50% position being axially aligned to a vane trailing edge. In the figures, an arrow aligned to the leading edge of a blade is used to define the vane-pitch of that blade. Each of the contour plots represents a "snapshot" of the instantaneous flow properties on the casing wall. The measurement area is divided into three distinct regions: the blade over-tip gap, the rotor passage and the vane–blade axial gap. The following discussion considers the flow phenomena in each of these distinct areas of the over-tip domain.

2.2. Over-tip casing heat transfer rate

This section describes the spatial and temporal evolution of the unsteady heat transfer to the casing wall. A physical explanation for these observations is developed in later sections that describe the static pressure and adiabatic wall temperature results.

The measured variation in casing heat transfer rate is presented in Fig. 3 as a sequence of eight contour plots at increments of blade phase that cover one blade passing cycle. At each time step the physical location of the nozzle guide vane trailing edges and the blade-tips are shown in outline. The data sequence shows that there are large spatial variations in the instantaneous heat flux to the casing wall, with these being associated with the circumferential position of the blades (vane-pitch). A region of high heat transfer is associated with the blade-tip gap, where the highest measured values of up to 320 kW/m^2 are observed. In contrast, the blade passage produces significantly lower heat transfer that gradually drops toward the blade trailing edge plane. In the vane–blade axial gap, a region of high casing heat flux is seen to track with the early blade suction surface with lower values immediately upstream of the blade passage inlet. All of these features are modulated (to varying degrees) according to the position of the blade-tips relative to the upstream vanes (i.e. as a function of vane-pitch). These features will be discussed in detail in the following sections. It is worth noting that these heat flux results show largely similar features to the data presented by Guenette et al. (1985), which also showed high heat transfer rates within the tip-gap and a generally falling trend through the stage.

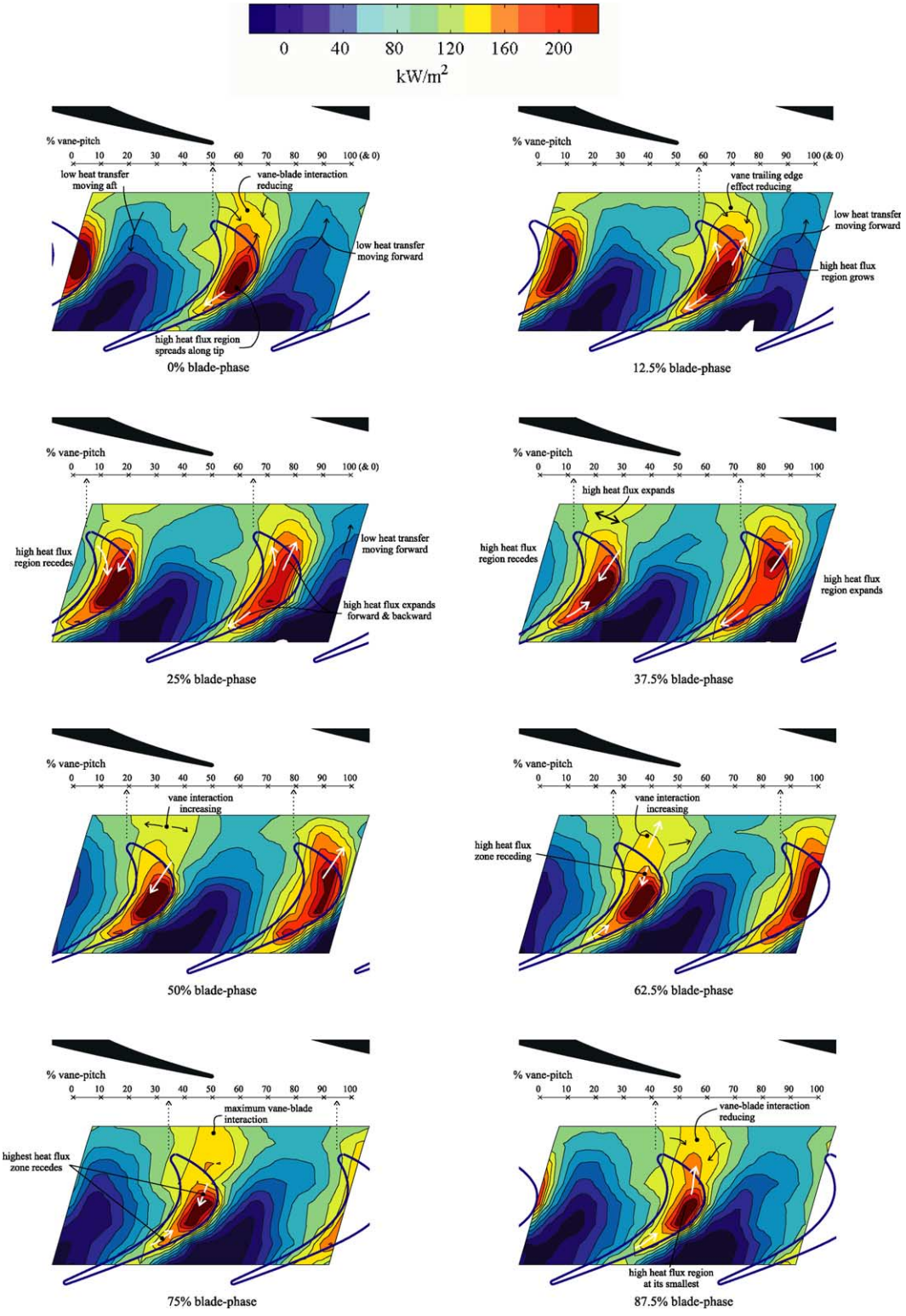

Fig. 3. The measured instantaneous casing wall heat flux distribution presented as a function of blade-phase.

2.2.1. Heat flux to the casing wall from the blade over-tip flow

As the suction surface corner of a blade-tip approaches and then passes over a particular point on the casing wall, the heat transfer rate increases sharply to a maximum value that can be in excess of 300 kW/m^2. This region of highest heat flux is seen in Fig. 3 to be associated with the crown region of the blade-tip at all

blade-phase values. In addition, the extent of this region is modulated according to the circumferential position of the blade-tip relative to the upstream vanes (vane-pitch) as will now be discussed. As a blade-tip translates from 50% to 100% vane-pitch the region of high heat flux within the tip-gap spreads both backward within the tip footprint, and forwards toward the early blade suction surface. As the blade-tip passes through 100% vane-pitch and begins a new cycle, this area of high heat flux within the tip-gap begins to shrink (see the 25% blade-phase plot in Fig. 3). As the tip progresses further around the annulus this continues until it reaches its smallest physical area at 40% vane-pitch (the contour plot at 87.5% blade-phase). At this point, the highest heat flux levels are concentrated toward the suction surface and near the crown of the tip profile. This cycle of events then repeats. The high heat flux region is generally contained within the over-tip gap between blade and casing, except on the early suction surface, where a region of high heat flux tracks with the tip. This is caused by a vane interaction that will be discussed in a later section.

The leading edge region of the blade-tip gap produces casing heat flux levels that are similar to those found immediately outside the tip-gap region. This is not surprising since the blade-lift in this region is low, and does not create a significant leakage flow such as is found further along the blade. Toward the trailing edge of the blade, heat transfer rates within the tip-gap are always below those found further forward. The heat flux within the tip-gap toward the trailing edge of the blade (between 65% and 80% rotor axial chord) shows a lower value than is the case further forward. However, this region too displays a periodicity that is associated with the blade position relative to the upstream vanes. This can be best appreciated by considering the yellow and orange contours in Fig. 3. The position at 0% blade-phase shows that this yellow contour level reaches approximately 65% rotor axial. As the blade-tip moves onward from this position the yellow contour moves along the tip toward the trailing edge, until at 62.5% blade-phase the tip at 86% vane-pitch shows the maximum downstream extent of this high heat flux. As the blade moves further around the annulus and starts a new vane-passing cycle, the yellow contour moves gradually forward along the blade-tip. These observations are consistent with vane-periodic changes in the static pressure distribution around the tip that are described in a subsequent section.

Overall, these measurements suggest that the heat flux produced as a blade-tip passes a particular point on the casing is greatly influenced by the local pressure difference across the blade-tip at that point. Indeed, the high heat flux levels within the over-tip region coincide with the regions of high blade lift. This theme is developed further in the section relating to static pressure measurements.

2.2.2. Heat flux to the casing wall from the rotor passage flow

Considering the sequence of contour plots presented in Fig. 3, the rotor flow is characterised by a generally falling instantaneous casing heat transfer rate as the flow passes through the blade row. Within this region, maximum heat transfer rates of approximately 100 kW/m^2 are evident at the rotor inlet plane, although this drops consistently to -20 kW/m^2 toward the rotor exit plane. Primarily, this reduction in the heat transfer can be attributed to the falling flow total temperature through the rotor. In addition to this, the instantaneous heat transfer to the casing wall within the rotor passage is modulated according to the vane-pitch of the passage in question. This can most easily be seen in the contour plot at 12.5% blade-phase in Fig. 3. In the blade passage at 90% vane-pitch the low levels of heat transfer (blue contours) are pulled forward to the front of the measurement domain, while the rotor passage at 30% pitch sees those levels further back within the passage.

2.2.3. Heat flux to the casing wall in the vane–blade axial gap

The data presented in Fig. 3 clearly shows that a significant disturbance to the casing heat transfer is produced in the vane–blade axial gap by the moving blades, this indicates the upstream propagation of a blade related flow disturbance. In general, this manifests itself as a region of high heat flux axially upstream of the early suction surface of a blade. This enhanced heat flux region tracks with the blade-tips as they move around the annulus and is modulated by the proximity of the upstream vanes, as will now be discussed. Considering the position at 0% blade-phase in Fig. 3, the region of high heat flux in the vane–blade gap is axially upstream of the blade and is receding back toward the tip. As the blade moves from 50% to 100% vane-pitch, this region initially moves back and then stabilises. At the same time, a region of higher heat transfer spills out from the blade-tip gap onto the early suction surface. As the blade position passes through 10% vane-pitch (see the contour plot for 37.5% blade-phase), a zone of high heat transfer begins to spread axially upstream, whilst at the same time the high heat flux in the tip-gap continues to shrink back away from the leading edge and early suction surface. This is related to the interaction between the blade and vane potential fields. The enhancement in heat transfer within the vane–blade gap is maximised at around 35% vane-pitch, wherein the vane interaction starts to reduce and the cycle repeats.

2.3. Over-tip casing static pressure

This section describes the unsteady casing wall static pressure measurements. This data is discussed in the context of developing a physical understanding of the unsteady aerodynamics of the turbine tip region, and thereby to propose physical mechanisms that aid the explanation of the casing heat transfer data. The measured variation in the instantaneous casing static pressure is presented in Fig. 4 as a sequence of contour plots that cover one blade passing cycle. These are at the same blade-phase increments as the heat flux data presented in Fig. 3. Overall, the data reveal the large spatial variations in instantaneous static pressure that are associated with the lift distribution produced by the blades. Whilst this is the predominant feature of the data at each blade-phase, the data also reveal more subtle variations related to the vane-pitch position of the blade-tip. In particular, this can be seen axially downstream of the vane trailing edge and along the early suction surface of the blade, where a region of high static pressure develops as the blade leading edge approaches and then passes. Within the blade-tip footprint, the acceleration of the flow into the tip-gap can be seen in the steep pressure gradient that develops along the pressure surface corner.

In the following sections this data is discussed in more detail. The interpretation is used to develop physical mechanisms that explain the complex relationships between aerodynamics and heat transfer.

2.3.1. Static pressure in the over-tip gap

The variation in the static pressure distribution within the blade-tip gap are visualised in the contour plots presented in Fig. 4. The variation of static pressure within the tip-gap is principally controlled by the blade loading distribution, which determines the pressure at a particular point around the blade profile. The resulting pressure difference between the two aerodynamic surfaces drives the tip-leakage flow through the 1.2 mm gap between blade-tip and casing wall. The presence of the tip-leakage modifies the pressure distribution around the blade in the region of the tip due to sink and source effects (Metzger and Rued, 1988; Rued and Metzger, 1988). The static pressure in the tip-gap is characterised by strong pressure gradients that run approximately normal to the blade pressure surface from about 30% axial chord. This is in contrast to the suction surface, where the static pressure gradient is approximately parallel to the local blade-tip profile up to 55% axial chord. Beyond this point, the pressure along the suction surface corner of the tip changes only slightly. This can be explained by the fact that the geometrical throat of the blade-row intercepts the suction surface at approximately 55% axial chord. In the vicinity of the tip leading edge the static pressure is not significantly different to the pressure of the flow immediately upstream and outside the tip-gap.

The static pressure in the tip-gap is modulated as a function of vane-pitch as the blade-tip moves around the annulus. In particular, the pressure contours near the early suction surface of the blade (between leading edge and crown) are significantly shifted by this periodic interaction with the upstream vane. The two extremes of this phenomena can be seen in the 50% and 87.5% blade-phase contour plots: when the tip leading-edge is at 80% vane-pitch the low static pressure contours are pulled forward along the suction surface, while at 40% vane-pitch they are pushed back. This change in the loading distribution on the forward part of the blade-tip changes the pressure difference across the tip, and causes a modification to the tip-leakage flow speed and direction. This has a significant impact on the unsteady heat flux to the casing: higher pressure difference produces higher casing heat flux and vice versa.

The measurements of the casing wall heat flux have established that the heat transfer occurring within the tip-gap is changed as a function of blade-tip position relative to the upstream vanes. The cause of this can now be seen to be related to the unsteady blade-lift.

Considering the situation as a blade-tip passes from 50% to 100% vane-pitch, it is clear that the static pressure distribution around the early suction surface of the blade is changed as the blade moves away from the vane trailing edge. This is revealed by the way in which the low static pressure contours move forward around the blade profile. To aid interpretation of the data, the black circles in Fig. 4 show where the particular contour lines intersect the blade-tip profile, and these can be tracked in the succession of contour plots. This advancement of the low pressure along the suction surface leads to an increase in the pressure difference between the aerodynamic surfaces and thus causes an increase in the leakage flow over this front portion of the tip. In addition, the flow direction within the tip-gap is adjusted (this has been found to produce variations in recovery temperature on the casing wall that are discussed later). The consequent effect on the casing heat flux is seen in Fig. 3, where the high heat flux zone within the tip-gap gradually moves forward as the lift on the early part of the blade increases. In the contour plot at 50% blade-phase, the blade-tip at 80% vane-pitch shows where the static pressure contours are at their most upstream location; this is also the point at which the high heat transfer in the tip-gap is pulled most toward the blade leading edge.

As the blade position advances through 100% vane-pitch, and starts a new vane passing cycle, the lift distribution on the early suction surface is gradually pushed back until at 26% vane-pitch a vane trailing edge interaction becomes a dominant effect. This is clearly seen in the static pressure contour plots at 62.5% and 75% blade-phase where a region of higher static pressure

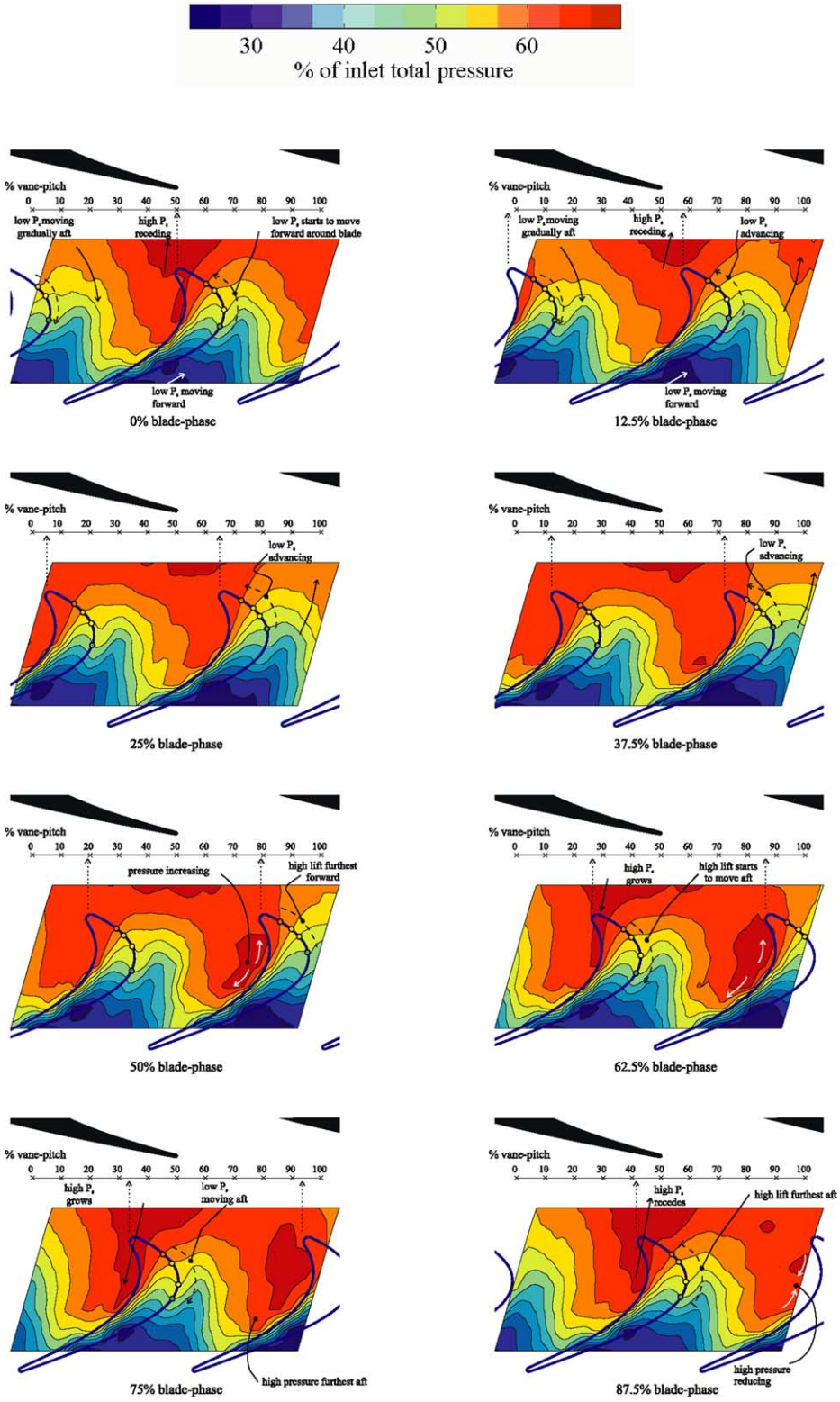

Fig. 4. The measured instantaneous casing wall static pressure distribution presented as a function of blade-phase.

suddenly penetrates through the tip-gap and onto the blade pressure surface. Simultaneously, the static pressure contours on the blade suction surface begin to migrate slightly further downstream away from the leading edge. This reduces the pressure difference across the upstream portion of the blade-tip and so causes a fall in the tip-leakage velocity. This reduction in blade-lift is responsible for a reduction in the casing heat flux within

the tip-gap as the blade moves from 0% to 40% vane-pitch, as can clearly be seen in Fig. 3. At 40% vane-pitch, the pressure difference across the tip is minimised and the extent of the high heat flux region is also minimised.

The movement of the static pressure contours under the influence of the upstream vanes is evident all along the suction surface. On the latter part of the blade, a modulation of the pressure difference across the tip can be seen in Fig. 4. In this region (from about 60% rotor axial chord) the static pressure on the suction surface of the blade is changed slightly according to the vane position of the tip. This is characterised by a region of slightly lower static pressure that starts to advance forward in the blade passage from about 50% vane-pitch. This dark blue region appears to reach the geometric throat of the blade passage by about 60% vane-pitch and then hold a constant position as the blade advances further round the annulus. As the blade starts a new vane passing cycle, the static pressure adjacent to the latter part of the suction surface increases slightly and remains in this state until the blade reaches 50% vane-pitch wherein the cycle repeats. Changes in the static pressure on the pressure surface of the blade are also evident on the latter part of the tip. This is particularly noticeable as the blade moves from 65% to 95% vane-pitch, as a region of higher pressure develops on the pressure surface and spreads downstream. This reaches its most downstream position at about 95% vane-pitch (the 75% blade-phase plot). This increases the local pressure difference across the blade-tip and, in conjunction with the smaller changes on the suction surface, causes an increase in the tip leakage flow. This can be seen in the heat flux measurements (Fig. 3) where the heat transfer to the casing on the latter part of the blade-tip increases when the blade is in the range 65–95% vane-pitch. At other positions, the heat flux is reduced owing to the reduced blade-lift at those positions.

2.3.2. Static pressure in the blade passage

The static pressure within the blade passage is characterised by a decreasing trend as the flow expands and accelerates in the blade-relative frame of reference. The measurements of the instantaneous pressure (Fig. 4) capture this basic aerodynamics as measured on the casing wall. These results show how the flow accelerates around the early suction surface and how the cross-passage pressure gradient is established. There are significant changes to this generalised view of the static pressure field that are caused by the interaction of the blade with the upstream vanes. These interactions have a significant effect upon the static pressure distribution around the blade that influence that heat transfer to the casing wall. As has already been observed, the static pressure distribution around the blade-tip drives the over-tip leakage flow, and any modification to this causes changes in the tip-aerodynamics and heat transfer.

The acceleration of the flow through the passage in the relative frame of reference leads to a reduction in the flow speed in the absolute frame because of the changing flow angle. Of course, the rotor reduces the angular momentum of the fluid to produce useful work. In the absence of other factors, this would be expected to lead to a reduction in the Nusselt number on the casing wall, as has been observed in the time-mean data (a fall of 36% between rotor inlet and 80% axial chord, Thorpe et al., 2004). However, the absolute total temperature of the flow is also reduced by the blade-row and this acts to establish a falling trend in the heat flux. Consequently, the passage flow is characterised by falling levels of heat transfer to the casing as the flow progresses through the rotor. This can be seen clearly in the heat flux measurements presented in Fig. 3.

The static pressure within the blade passages is affected by the presence of the upstream vanes. This is manifested in the form of a vane-periodic migration of the pressure contours within the passage as the blades rotate. Considering the position at 25% blade phase in Fig. 4, it is apparent that the two blade passages shown have subtly different pressure distributions. In the entrance to the passage at 100% vane-pitch, the low static pressure contours are further forward toward the vane exit plane. In contrast, the left-hand passage has higher static pressure at its inlet, and the static pressure contours are pushed back toward the blade trailing edge (this is particularly evident in the yellow contour lines). The consequent changes to the casing heat flux can be seen in Fig. 3: the contours of constant heat flux in the passage at 100% vane-pitch are pulled upstream compared to those in the left-hand passage.

2.3.3. Static pressure in the vane–blade axial gap

The region between vane exit and rotor inlet—the vane–blade axial gap—is known to exhibit complex unsteady phenomena that are associated with the high Mach number flow from the vane and the periodic blade passing immediately downstream. Recent publications (for example, Miller et al., 2003; Denos et al., 2001) have given considerable insight into these unsteady interaction effects. The interaction involves three primary physical mechanisms: firstly, the modulation of the static pressure field according to the blade position, the so-called potential field interaction; secondly the presence of the vane trailing edge shock system; and thirdly, the velocity and total pressure deficits in the vane wake. The evidence of such effects is apparent in the measured casing static pressure distribution presented in Fig. 4. Generally, the vane trailing edge (at 50% vane-pitch) is associated with a region of higher static pressure that shifts and intensifies under the influence of the moving downstream blades. Away from the vane trailing edge,

the static pressure in the vane–blade axial gap is also influenced by the blade potential field which causes fluctuation in the local static pressure. These complex interactions will now be considered in more detail.

Considering the instantaneous static pressure within the vane–blade axial gap at a blade-phase of 0% (Fig. 4), a region of higher static pressure extends from the vane trailing edge, through the tip-gap and along the blade pressure surface. At this point in the blade passing cycle, this area of high pressure is moving axially toward the vane trailing edge. As the blade moves away from this position, the region of higher static pressure recedes further and eventually becomes a small feature concentrated at −20% rotor axial chord (the limit of the measurement domain). This position remains largely unchanging until a blade approaches the 25% vane-pitch position (the 62.5% blade-phase plot in Fig. 4) wherein a sudden rise in static pressure projects from the vane trailing edge region, through the tip-gap and onto the blade pressure surface. This suggests the presence of a shock (or succession of small compression waves) that form due to the reducing effective throat area between the vane trailing edge and blade leading edge. The area affected by this high static pressure increases axially at 75% blade-phase. It can also be appreciated that this shock interaction is responsible for a further change in the static pressure on the early suction surface, as commented on in an earlier section about the static pressure in the tip-gap. The effect of these changes can be seen in the heat flux data in Fig. 3. As a blade approaches the vane trailing edge (50% blade-phase) the region of high heat flux axially upstream of the early suction surface begins to extend further toward the vane trailing edge. This feature intensifies as the blade leading edge approaches the vane trailing edge (87.5% blade-phase) and then begins to diminish as the blade leading edge moves away from the vane trailing (0% blade-phase). The cause of the locally increased heat transfer as a blade passes near the vane trailing edge is considered to be an increase in the local heat transfer coefficient and an increase in the flow total temperature that is produced by a compression (discussed later).

2.4. Over-tip casing adiabatic wall temperature

The static pressure measurements have revealed the influence of the tip-region aerodynamics on the unsteady heat transfer to the casing wall. This is dominated by the variation of work production through the rotor that leads to large spatial variations in the instantaneous total temperature distribution. The distribution of work in the blade-passages causes temporal variations in the absolute flow velocity and pressure (and hence Nusselt number on the casing wall) and the adiabatic wall temperature: both of these parameters cause changes in the casing heat flux. This section explores the latter of these two influences through the measurements of unsteady adiabatic wall temperature, and in particular, how this relates to the aerodynamics and heat transfer processes that are occurring on the casing wall.

The time-resolved adiabatic wall temperature (recovery temperature) has been measured for 40 of the 56 heat transfer gauge positions. This unique data has enabled the temporal and spatial variations in heat transfer driver temperature to be established. Unfortunately, this type of data was not collected for 16 of the heat transfer gauge locations, and because of this it is impossible to display the data in exactly the same way as has been done for the heat flux and static pressure. In addition, it is not possible to analyse the detailed vane–blade interaction effects. However, this information is still extremely useful in gaining an understanding of the complex nature of the tip-leakage environment. Presented in Fig. 5 is a sequence of contour plots of the measured time-resolved adiabatic wall temperature for one complete blade passing cycle (note that the data is restricted to three complete columns of gauge positions). These are at the same blade phase increments as the heat flux and static pressure measurements presented in Figs. 3 and 4.

The striking features of the data are the high temperatures present within the tip-gap and the rapidly falling temperatures as the flow progresses through the rotor passage. In fact, the maximum measured temperatures within the tip-gap are above the stage inlet total temperature and indeed these unique results have indicated the presence of a work process that acts upon the tip leakage fluid (this is discussed subsequently). The principal features in the data are seen to track with the blade-tips on the succession of plots. It is immediately apparent that there are strong temporal variations in the adiabatic wall temperature at all measurement locations, including upstream of the rotor leading edge in the vane–blade axial gap. At around 60% rotor axial chord, the size of this fluctuation is in excess of 100 K at the blade passing frequency of 8.9 kHz. Overall, the data show similar spatial features to the heat flux measurements presented in Fig. 4: this is to be expected since the instantaneous heat flux is directly dependent upon the local recovery temperature. From this it can be seen that the unsteady heat flux is significantly influenced by the large flow temperature changes that occur at the blade passing frequency. Furthermore, in the light of this data it can be appreciated that a full assessment of the heat flux data presented in Fig. 3 can only be achieved if the unsteady adiabatic wall temperature is also available for analysis.

The measurement of the unsteady adiabatic wall temperature through the turbine is additionally useful since it is closely related to the flow total temperature, and therefore reveals details of the aerodynamic work processes that occur adjacent to the over-tip casing wall.

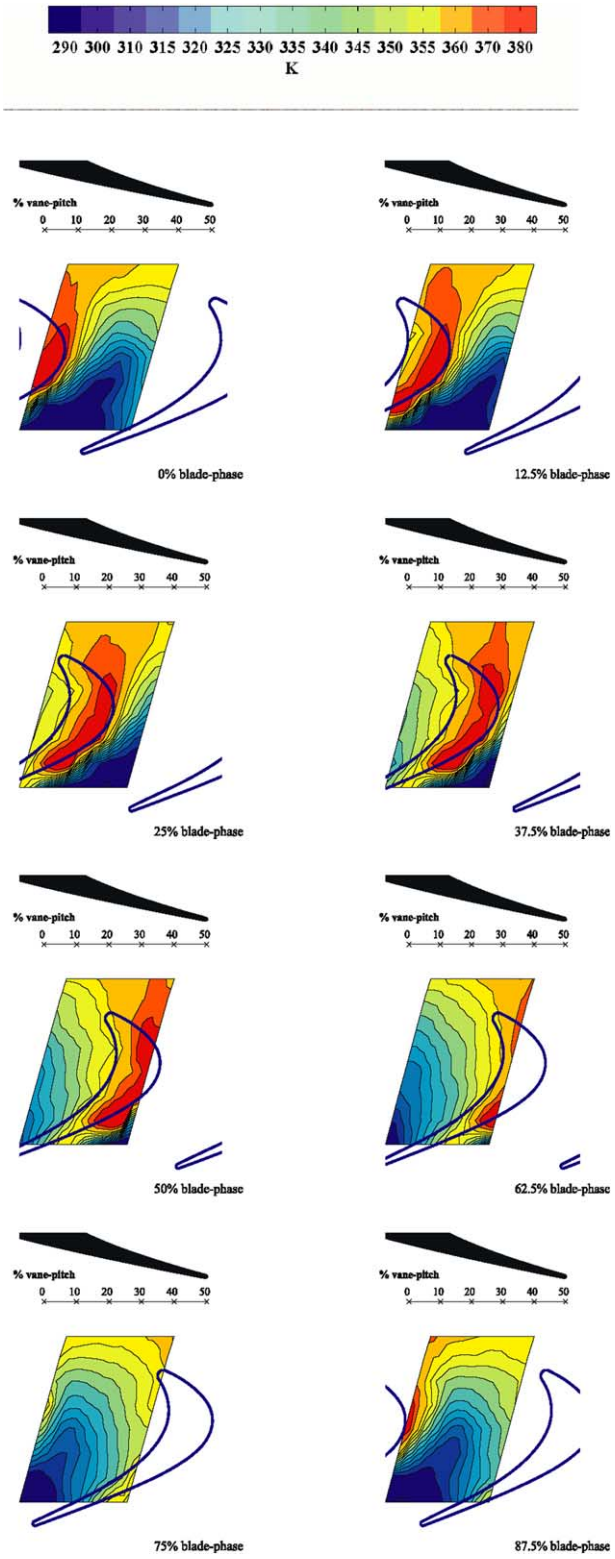

Fig. 5. The measured instantaneous casing wall adiabatic wall temperature distribution presented as a function of blade-phase.

In this way, the data can be used to provide additional insight into the aero-thermodynamics of the turbine. Of course, the adiabatic wall temperature on the casing wall is slightly below the absolute flow total temperature, but is related to it through the local temperature recovery factor and Mach number. The difference between these two temperatures is 2% (9 K) at a Mach number of 0.93 and total temperature of 374 K (the vane exit Mach number in these experiments).

2.4.1. Adiabatic wall temperature in the blade over-tip flow

Considering the data presented in Fig. 5 it is apparent that the blade tip-gap is characterised by a region of elevated adiabatic wall temperature that is highest toward the suction surface corner of the tip profile. The region of highest temperature (the red contour in Fig. 5) is generally confined to a region between the mean camber line and the suction surface corner. This region is mostly contained within the tip footprint, except along the early suction surface of the blade where high temperatures are seen to extend axially upstream into the vane–blade axial gap. The high temperatures within the tip-gap are seen to coincide with regions of high heat flux (Fig. 3), as might reasonably be anticipated. This clearly demonstrates that the high levels of heat transfer are intimately linked to the unsteady temperature field. Referring to the static pressure data of Fig. 4, it can be seen that the high adiabatic wall temperatures in the tip-gap flow coincide with regions of high blade-lift; that is, where the pressure difference across the tip is highest.

The temperature in the tip-gap near the leading edge of the blade-tip is not significantly different to that immediately outside the tip-gap. The static pressure measurements have indicated that the pressure difference across the blade-tip is small in this region, and can presumably only drive modest levels of tip-leakage flow. The fact that the temperature here is not strongly affected by the presence of the blade-tip appears consistent with the argument that the leading edge region of the blade-tip causes relatively small time-varying changes in the aerodynamics adjacent to the casing wall. Indeed, the heat flux data presented in Fig. 3 confirms this.

In general, the temperature gradients near the pressure surface are significantly smaller than are seen along the suction surface. Toward the blade trailing edge, temperatures within the tip-gap are still above those found in the blade passage at the same axial location, but are reduced compared to the values seen further forward on the tip.

The measured instantaneous adiabatic wall temperatures within the tip-gap can exceed the turbine stage inlet total temperature by as much as 35 K (the stage inlet total temperature being 374 K in these experiments). This surprising result implies the presence of a work process that acts on the tip-leakage flow, thereby increasing its stagnation temperature in the absolute frame of reference. Consequently, the instantaneous

heat transfer driver temperature within the tip-gap rises above that seen elsewhere on the casing wall. This is the first time that the existence of such a work process has been suggested. However, the fact that work is done on the over-tip leakage fluid is particularly significant for the heat transfer that occurs to the stationary casing wall. It suggests that the high heat flux observed within the tip-gap is caused by two physical effects: firstly the increase in heat transfer coefficient produced by the disturbance of the casing boundary layer; and secondly the increase in flow recovery temperature. Further discussion of this important point will be presented in a later section.

2.4.2. Adiabatic wall temperature in the rotor passage

The instantaneous adiabatic wall temperature within the rotor passage can be seen in the sequence of contour plots in Fig. 5. At the rotor inlet plane the temperature is in the range 360–370 K, and displays a spatial periodicity that is clearly associated with the blade position. As the flow enters the rotor passages the temperature is seen to drop in the centre of the passage and then adjacent to the suction surface of the blades. At a given axial position, the adiabatic wall temperature near the blade pressure surface is always higher than elsewhere in the rotor passage. As the flow continues toward to the rotor exit plane the temperature drops further to approximately 300 K.

In general, the variation of adiabatic wall temperature within the blade passages closely resembles the distribution of heat flux presented in Fig. 3. At a qualitative level this is not a surprising result, but does serve to reinforce a key finding in this work: that the unsteady temperature field is a significant influence on the unsteady casing heat flux.

The general features of the distribution of recovery temperature in the blade passages can be explained by consideration of the flow in the absolute frame of reference. At inlet to the rotor passages the flow velocity is high (around 300 m/s) and has a large circumferential component that is imparted by the nozzle guide vanes. The flow recovery temperature here is close to the stage inlet total temperature: this has been clearly demonstrated in Part I of this work (Thorpe et al., 2004). As the fluid enters the blade passages it starts to be turned toward the axial direction and is slowed in the absolute frame of reference. The consequent loss of angular momentum is of course the source of work produced by the rotor. It is also the mechanism by which the absolute total temperature of the flow is reduced through the stage as work is extracted. This is clearly evident in the data presented in Fig. 5 for the flow in the blade passage. Previous discussions have indicated that the adiabatic wall temperature can be used to assess the flow total temperature. In fact, the contour plots in Fig. 5 can be used to visualise the parts of the flow field that have done work, in other words, regions where the angular momentum of the fluid has been reduced compared to the nozzle guide vane exit condition.

2.4.3. Adiabatic wall temperature in the vane–blade axial gap

Upstream of the rotor inlet plane, spatial variations in the instantaneous adiabatic wall temperature can clearly be seen, and are related to the blade position. At −20% rotor axial chord for instance, the magnitude of this temperature fluctuation is 20 K. Particularly interesting is a region of high temperature that extends axially upstream from the blade-tip/suction surface corner. This region was seen in Fig. 3 to also have an elevated casing heat flux. One cause of this high heat transfer is clearly the increased local flow recovery temperature. At the entrance to the blade passage (see the 75% blade-phase plot in Fig. 5) the adiabatic wall temperature is significantly lower than immediately in front of the blade-tip. Likewise, the heat flux as the flow enters the blade passage is also reduced. If we now interpret the unsteady adiabatic wall temperature on the casing as unsteady total temperature, it is apparent that there is an unsteady work process that changes the flow conditions as the blades move relative to the guide vanes.

3. Further discussion

From a turbine design point of view, a knowledge of the time-mean heat load imposed upon the casing wall is of critical importance. It is this parameter that determines the required cooling regime and the metal temperature. However, as the data presented here shows, the time-mean level is caused by a massively time-dependent heat flux that is dictated by the turbine design, including factors such as blade loading distribution and tip-gap height. Consequently, the estimation of the casing heat load requires an appreciation of the complex aero-thermodynamics, both for the passage flow and the tip-leakage flow. This appreciation has two significant benefits for the engine designer: firstly an ability to predict heat transfer in the engine environment and thereby establish a design rapidly; secondly, a physical understanding that promotes design innovation and improvements. The unique time-resolved data presented here has suggested that the flow conditions adjacent to the casing wall can be broken into two distinct regimes: firstly that associated with the rotor passage flow and secondly that associated with the over-tip leakage flow. Of these, the over-tip leakage flow contributes a proportion of the casing heat load that can be considered an unnecessary burden, while the heat load originating from the passage flow is largely unavoidable.

3.1. The significance of over-tip leakage on the casing heat load

The data and discussion presented in previous sections have indicated that the factors which affect the casing heat load can be divided into two distinct parts: those related to the passage flow-field and those related to the over-tip leakage flow-field. For instance, if we consider a particular point on the over-tip casing wall, there is a certain fraction of the blade-passing period during which a blade-tip is directly over-head, while for the remaining time it is the blade passage flow. Clearly, in a shroudless design the blade passage flow is always exposed to the stationary casing, and in that sense the casing heat load from the passage flow is largely unavoidable. In contrast the tip-leakage flow is an entirely undesirable consequence of the shroudless design that is known to have a negative impact upon several aspects of the turbine performance, including the overall stage efficiency. The data presented here also suggests that the tip-leakage fluid has a strong adverse effect on the casing heat load. Indeed, the tip-gap flow yields the highest instantaneous heat flux to the casing and can contribute up to half of the time-mean heat load.

In order to quantify the impact of the tip leakage flow on the casing heat load, the time-resolved data presented previously has been divided into passage flow and over-tip flow sections. A graph to illustrate the analysis procedure is presented in Fig. 6. It shows a graph of the typical heat transfer rate at a point on the casing as a function of the blade-passing cycle. The time during which a blade-tip is directly above the measurement location is indicated in Fig. 6. For this data we can integrate the heat flux in each region (the tip flow and passage flow) and thereby estimate the relative size of the heat load originating from each. The result of this exercise is presented in Fig. 7 as a function of axial position through the blade row. Note that upstream of the rotor there is no tip-leakage contribution to the heat load. The heat load originating from the rotor passage flow is seen to fall through the stage, rapidly up to 35% rotor axial chord and then more slowly toward the rotor trailing edge. In contrast, the casing heat load produced by the tip-leakage flow increases from the leading edge to 35% axial chord and then decreases. Around the blade mid-axial chord, approximately half of the casing heat load is produced by the tip-leakage flow, despite the fact that in the circumferential direction the blade thickness is 3.4 times smaller than the passage width. It is worth noting that this approach to assessing the contribution of the tip leakage flow to casing heat load is probably a conservative estimate, since it is based purely on the physical "footprint" of the tip, whereas in actuality the tip-leakage flow also has a significant impact in the passage due to the tip-leakage vortex. The cause of this behaviour can be revealed by analysing the adiabatic wall temperature and Nusselt number in the same way as has been done for the heat load, that is, by dividing the data into tip and passage flow regions and averaging each. Presented in Fig. 8 is a graph of mean adiabatic wall temperature for the tip-flow and passage flow as a function of axial position. The adiabatic wall temperature in the blade passage falls consistently through the blade-row as work is extracted by the rotor. In contrast, the temperature of the tip-leakage flow initially increases to a maximum value at 35% axial chord and then falls quite rapidly toward the trailing edge. In Fig. 9, the average Nusselt number in the two flow regimes is presented. This again indicates a falling trend for the passage flow as the flow is decelerated and expanded through the rotor. In fact, the average Nusselt

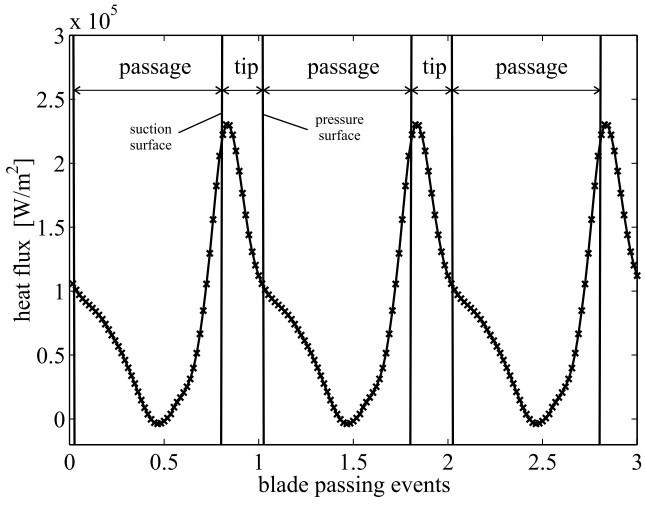

Fig. 6. A graph that illustrates how the time-resolved heat flux data can be divided into passage and tip flow regions.

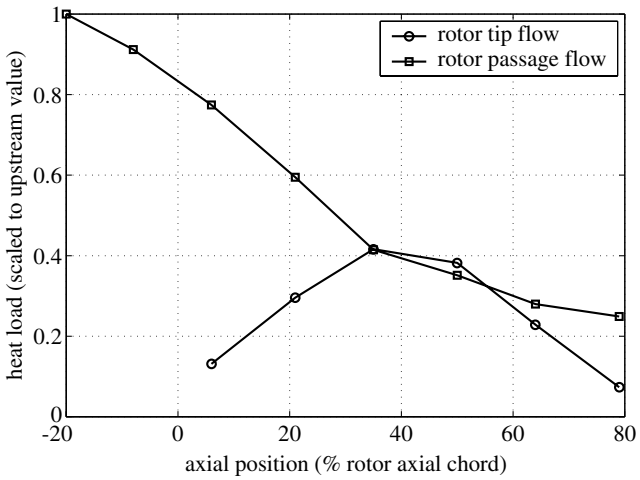

Fig. 7. A graph showing the measured casing wall heat load as a function of axial position through the rotor.

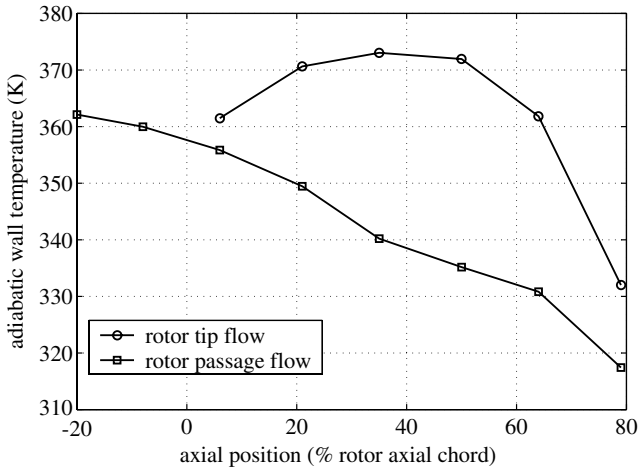

Fig. 8. A graph showing the measured variation of adiabatic wall temperature for the tip-leakage flow and blade-passage flow as a function of axial position.

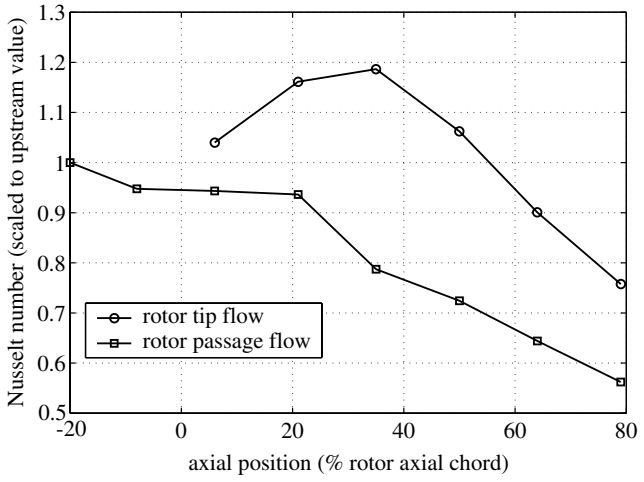

Fig. 9. A graph showing the measured variation in casing wall Nusselt number for the tip-leakage and blade-passage flows as a function of axial position.

number in the passage falls by 40% between 0% and 80% rotor axial chord. In contrast, the Nusselt number in the tip-leakage flow is seen to be maximised at 35% rotor axial chord and then to exhibit a decreasing trend toward the trailing edge of the blade.

It is apparent that the adiabatic wall temperature and heat transfer coefficient are both high in the tip-gap when compared to the values in the blade passage at the same axial location. The increase in the adiabatic wall temperature is associated with a work process that acts on the tip-leakage fluid, and this effect is seen to be maximised around the mid-axial chord position. The heat transfer coefficient is increased within the tip-gap by the high absolute flow velocities and the periodic disruption of the casing boundary layer.

3.2. Interpretation of the data: work processes in shroudless turbine rotors

The measurements presented in this article have indicated the presence of a work process that increases the absolute stagnation enthalpy of the over-tip leakage fluid. This has been deduced from the observations of high instantaneous adiabatic wall temperatures on the casing wall as a blade-tip passes over that point. This also represents an increase in flow total temperature in the absolute frame of reference. An undesirable consequence of this work process is that it causes an increase in the time-mean flow recovery temperature on the casing wall, and can thus lead to higher heat flux and metal temperatures. It is therefore appropriate to formulate the physical mechanisms that are responsible for this work process before going on to the direct effect on the casing heat load.

The work produced by a turbine rotor is related to the change in angular momentum of the fluid passing through it. Presented in Fig. 10 are the velocity triangles for the rotor inlet and exit planes as well as a hypothesised velocity triangle for the tip leakage fluid. It is apparent that the direction of the over-tip leakage flow is significantly different to that of the flow in the blade passage. In fact, the leakage fluid can have an absolute circumferential velocity that is above that at rotor inlet, indicating that work is done on this fluid and that its total temperature will be above that at inlet to the blade passage. In contrast, the fluid moving through the rotor passage has a circumferential velocity component that is less than that at inlet, and consequently has a stagnation temperature that is below that at blade inlet. The leak-

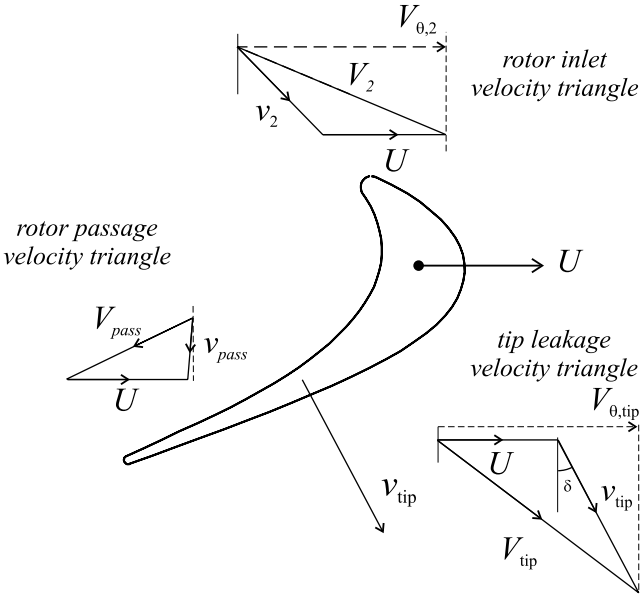

Fig. 10. A schematic diagram that illustrates the velocity triangles for the blade inlet, blade passage and over-tip leakage flows.

age flow is driven by the large pressure ratio (up to 1.9 in this case) across the blade-tip that is produced by the aerofoil lift distribution. Over the high lift portions of the blade (around mid-axial chord) the leakage fluid can achieve sonic velocities in the relative frame of reference, and at a flow angle that has a positive component in the direction of blade movement. Depending upon the flow direction, this can translate into very high velocities in the absolute frame (perhaps as high as Mach 1.5) and an increase in angular momentum relative to the blade inlet condition. This effect is clearly sensitive to the specific design of the turbine, and in particular the blade loading distribution. In order to estimate the temperature fluctuations, a simple model of this process has been derived. Considering the velocity triangles in Fig. 10, the vane exit flow is at a velocity of V_2 and an angle α_2 to the machine axis while the blade speed is U. The direction of the leakage flow in the blade-relative domain is δ, as indicated in Fig. 10. Applying the energy equation and assuming that the relative total temperature is constant through the rotor blade row, it can be shown that the change in stagnation enthalpy is given by Eq. (1).

$$H_{o,tip} - H_{o,2} = U(U + v_{tip}\sin\delta) - UV_2\sin\alpha_2 \quad (1)$$

The rise in stagnation temperature associated with the over-tip leakage work process can be estimated by employing the above equation between the rotor inlet plane and a particular point on the blade-tip. In Fig. 11 an example flow vector in the tip-gap is considered, and the corresponding rise in total temperature estimated. Of course this example refers to the flow conditions in the Oxford rotor facility. In the engine situation, the blade speed and sonic velocity are 50–100% higher. Eq. (1) indicates that if these results were scaled to the appropriate turbine entry temperature a recovery temperature fluctuation of 200–400 K would be observed.

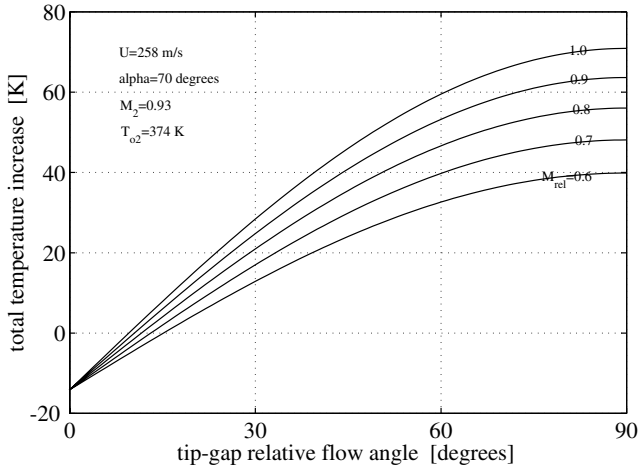

Fig. 11. A graph that illustrates the increase in absolute total temperature in the tip-leakage flow as a function of flow speed and direction.

3.3. Design implications

This section considers some of the wider implications of the work presented here. The purpose of this article is to provide a detailed understanding of the unsteady flow physics that influences the over-tip casing heat transfer field. As has been described, the role of the steady and unsteady blade-tip aerodynamics, particularly the unsteady blade lift, is vital to this endeavour. The results and understanding produced by this investigation can influence the turbine design process through two primary routes. Firstly, establishing the variation in non-dimensional heat transfer rate (Nusselt number) through the blade row for a turbine case that has received extensive investigation of flow conditions, and so allowing the estimation of the heat load for the engine environment. Secondly, the detailed analysis of the data has established an understanding of the complex flow physics that can promote design innovation and improvement.

The time-resolved casing wall measurements have enabled the sources of the casing heat load to be established and quantified. This unique data has indicated that the over-tip leakage flow can contribute up to half of the total heat transfer that occurs to the casing wall. The cause of this has been seen to be a higher Nusselt number in the tip-gap and a higher flow recovery temperature. This high temperature is caused by a work process that increases the angular velocity of the leakage fluid. The design of the blade, and the incorporation of blade-tip treatments, can influence the magnitude of the tip leakage velocity and also its direction. Such consideration might yield reduced casing heat load due to tip leakage. A design should be avoided if it is likely to produce strongly circumferential tip leakage flows, since this will yield high recovery temperatures on the casing wall.

4. Conclusions

The spatial distributions of over-tip casing heat transfer rate, adiabatic wall temperature and static pressure have been measured successfully in the Oxford University transonic axial turbine test facility. The unsteady heat flux to the casing wall was found to be strongly affected by the blade-passing events, with highest values measured within the tip-gap. Generally falling levels of casing heat transfer were found as the flow passes through the blade passage; this trend was found to be associated with decreases in flow total temperature and heat transfer coefficient. This overall picture was found to be modulated by the position of the blade-tips relative to the upstream vanes. The measurements of unsteady static pressure on the casing wall were used to develop a detailed understanding of the unsteady aerodynamics in the tip region, and to determine how these influence the unsteady heat flux to the casing wall.

Indeed it has been shown that the vane exit flow features cause a change in the blade loading distribution that produces a change in tip-leakage characteristics. A corresponding change in the unsteady casing heat transfer was also seen in the measurements. The data has been analysed so as to determine the heat load originating from the passage flow and the tip-leakage flow, and thereby to assess the relative importance of each. Some key points are summarised below:

- The over-tip casing heat transfer rate has a large unsteady component that is associated with blade-passing events. The magnitude of this fluctuation is highest around mid-axial chord, although the blade passing influence is seen at all axial positions, including upstream of the rotor inlet plane.
- A vane-periodic variation in blade-lift leads to changes in tip-leakage flow characteristics. This leads to associated changes in heat flux to the casing wall within the tip-gap due to fluctuations in velocity (heat transfer coefficient) and flow temperature.
- A work process acts on the tip-leakage fluid and causes its absolute total temperature to be increased, leading to high adiabatic wall temperatures within the tip-gap. Indeed, the absolute total temperature of the tip-leakage fluid can be above that at inlet to the turbine stage. This has a significant adverse impact on the casing heat load. A simple model of the tip-leakage work process has been developed.
- The fluctuation in blade-lift is associated with the vane exit flow conditions and interaction between moving and stationary components. The vane trailing edge shock system and potential field interaction have been seen to cause strong changes in static pressure along the suction surface of the blades. This change in pressure difference across the blade yields a time-varying pressure ratio across the tip, and thus a time varying leakage through the tip-gap. This complicated aerodynamic regime has been seen to cause corresponding changes in the unsteady casing heat flux.
- At a particular point on the casing, the total heat load can be considered to originate from two distinct flow regimes: the blade over-tip leakage flow and the blade passage flow. Analysis of the time-resolved data has indicated that up to half of the heat load comes from the over-tip leakage flow.
- The use of an engine representative facility has allowed significant new insight into features of the over-tip casing flow physics that have not previously been observed. In particular, this experimental approach has revealed the unsteady vane-rotor interaction and how this affects the pressure distribution around the blade tip and within the blade-tip gap. The presence of the vane trailing edge shock and the unsteady work processes have been identified in the aerodynamics measurements and used to explain the observations in unsteady heat transfer to the casing. The high-speed testing has also led to the discovery of a new physical mechanism, the so-called tip-leakage work process. In addition, the correct scaling of the aero-thermal conditions found in a modern gas turbine has provided non-dimensional heat transfer data (Nusselt number based on local adiabatic wall temperature) that can be scaled to the high-temperature engine situation, and is therefore of direct significance to engine design.

Acknowledgements

The support of Rolls-Royce plc and the Department of Trade and Industry is gratefully acknowledged. The authors would also like to acknowledge the generous support provided to Shin Yoshino by the Tokyo Electric Power Company (TEPCO). In addition, the experimental programme would not have been possible without the technical expertise of Mr. K.J. Grindrod and Mr. N.J. Brett.

References

Ainsworth, R.W., Schultz, D.L., Davies, M.R.D., Forth, C.J.P., Hilditch, M.A., Oldfield, M.L.G., Sheard, A.G., 1988. A transient flow facility for the study of the thermofluid-dynamics of a full stage turbine under engine representative conditions. American Society of Mechanical Engineers paper number 88-GT-144.

Denos, R., Arts, T., Paniagua, G., Michelassi, V., Martelli, F., 2001. Investigation of the unsteady rotor aerodynamics in a transonic turbine stage. Transactions of the American Society of Mechanical Engineers, Journal of Turbomachinery 123 (1), 81–89.

Garside, T., Moss, R.W., Ainsworth, R.W., Dancer, S.N., Rose, M.G., 1994. Heat transfer to rotating turbine blades in a flow undisturbed by wakes. American Society of Mechanical Engineers paper number 94-GT-94.

Guenette, G.R., Epstein, A.H., Norton, R.J.G., Yuzhang, C., 1985. Time resolved measurements of a turbine rotor stationary tip casing pressure and heat transfer field. AIAA paper number 85-1220.

Metzger, D.E., Rued, K., 1988. The influence of turbine clearance gap leakage on passage velocity and heat transfer near blade tips. Part I: sink flow effects on blade pressure side. American Society of Mechanical Engineers paper number 88-GT-98.

Miller, R.J., Moss, R.W., Ainsworth, R.W., Harvey, N.W., 2003. Wake, shock and potential field interactions in a 1.5 stage turbine. Part I: vane–rotor and rotor–vane interaction. Transactions of the American Society of Mechanical Engineers, Journal of Turbomachinery 125 (1), 33–39.

Rued, K., Metzger, D.E., 1988. The influence of turbine clearance gap leakage on passage velocity and heat transfer near blade tips. Part II: source flow effects on blade suction side. American Society of Mechanical Engineers paper number 88-GT-99.

Schlichting, H., Gersten, K., 2000. Boundary layer theory, 8th ed. Springer, Berlin. pp. 645–646.

Thorpe, S.J., Yoshino, S., Ainsworth, R.W., Harvey, N.W., 2004. An investigation of the heat transfer and static pressure field on the over-tip casing of a shroudless transonic turbine rotor at engine representative flow conditions. (I). Time-mean results. International Journal of Heat and Fluid Flow vol. 25, doi:10.1016/j.ijheatfluidflow.2004.02.027.